Turbulent flux parameterizations (The COARE Algorithm)

Parameterizations of turbulent fluxes at the air-surface interface are done employing the Monin-Obukhov similarity theory (MOST), which provides scaling relationships between the surface value of the turbulent fluxes and profiles of mean (and higher order) variable of the system. The turbulent fluxes are cross correlations of vertical velocity fluctuations (w') and fluctuations of other atmospheric constituents (horizontal wind, u', temperature, T', humidity, q', and any other variable, x'). In MOST, simple scaling parameters are computed from the fluxes

$$x_* = -\overline{w'x'} / u_*; u_* = -\overline{w'u'} / u_*$$

According to MOST, any property of the system driven by surface turbulence can be represented by a dimensionally appropriate combination of the scaling parameters and a single function of the dimensionless variable ζ

$$\zeta = \frac{\kappa g z}{T} \frac{\overline{w'T'} + 0.61T\overline{w'q'}}{u_*^3} = z / L$$

Here κ=0.40 is the von Karman constant, g the acceleration of gravity, z the height above the surface, and L the Monin-Obukhov stability length.

We can apply the MOST hypothesis to the vertical gradient of some mean atmospheric property as follows

$$\frac{\partial X}{\partial z} = \frac{x_*}{\kappa z}\phi_x(\zeta) = -\frac{\overline{w'x'}}{u_*\kappa z}\phi_x(\zeta)$$

In this case, ϕ_x is the dimensionless gradient function of z/L described above. The significance for the parameterization of surface fluxes becomes more apparent when this expression is integrated in height

$$X(z) - X_o = -\frac{\overline{w'x'}}{\kappa u_*}[\log(\frac{z}{z_{ox}}) - \psi_x(\zeta) + \psi_x(\zeta_o)]$$

Here X_o is the surface (interface) value of x realized at some roughness height, z_{ox}, and ψ an integral form of ϕ. The log-term describes the so-called *neutral profile* and the ψ function the effects of buoyancy on turbulent transport as represented by the stability length. This expression is only valid in the part of the profile dominated by turbulent transport; very near the interface

(i.e., mm scales) molecular transport becomes important and alternative expressions are used. Thus, z_o is not a physical variable of the system but the height where the extrapolation of the above expression intercepts the surface value of X; $\psi(\zeta_o) \approx 0$ and is usually neglected.

We can now write the surface fluxes in deceptively simple forms

$$\overline{w'x'} = C_x S(z)[X_o - X(z)]$$

where S is the wind speed computed from U and V components

$$S^2 = \overline{U^2 + V^2} = \overline{U^2} + \overline{V^2} + V_G^2$$

and V_G is a gustiness parameter that represents fluctuations in the wind components. We use these expressions for X= U, V, T, q, or some other atmospheric constituent exchanged between the air and the surface where

$$C_x = \frac{\kappa}{\log(z/z_o) - \psi_u(\zeta)} \frac{\kappa}{\log(z/z_{ox}) - \psi_x(\zeta)}$$

C_x is referred to as the bulk transfer coefficient. For historic reasons, wind constitutes a special notational case so that $C_{x=u}$ is written as C_d and called the drag coefficient and the velocity roughness length is written simply as z_o (i.e., the subscript *u* is dropped). Note that C_x is a function of both height and stability. For reference purposes, it is common to report the value for neutral conditions at z=10 m

$$C_{d10n} = \frac{\kappa}{\log(10/z_o)} \frac{\kappa}{\log(10/z_o)}; C_{h10n} = \frac{\kappa}{\log(10/z_o)} \frac{\kappa}{\log(10/z_{oT})}$$

where C_{h10n} refers to the 10-m neutral sensible heat transfer coefficient.

The inputs to our parameterizations are the basic bulk variables: the surface values (X_o) and the atmospheric values at some reference height ($X(z_r)$). These are either measured, determined in a model, or otherwise specified. The MOST stability functions are considered *universal*, i.e., they are determined experimentally in ideal conditions and then applied everywhere. The gustiness is usually represented in terms of boundary-layer scale variability; it is only significant at lower wind speeds. Most of the action is in the specification of the surface properties, either expressed as the roughness lengths or the 10-m neutral transfer coefficients. These obvious depend greatly on the nature of the surface: ocean, ice/snow, or vegetation and on the nature of the flux (momentum, heat, evaporation, gases, particles, etc). The basic algorithm described here was developed as part of the TOGA COARE field program in the tropical western Pacific. It includes components to handle the combined turbulent and molecular transfer

processes in the atmosphere and the water. The COARE algorithm was extended to the sea ice case for the SHEBA project over the Arctic icecap by changing the roughness specifications. It was then extended to gas transfer as part of the GASEX program. The same structure can be applied to simple overland situations, but this model is not well adapted to conditions with complicated vegetation and soil moisture interactions.

1. Air-Sea Fluxes

1.1. The COARE Bulk Flux Algorithm

1.1.1. History and Description

*In 1993, Chris Fairall, Frank Bradley and David Rogers began development of a bulk air-sea flux algorithm for use by the COARE community. Based on the model of Liu, Katsaros and Businger (1979, LKB), it took account of the light wind, strongly convective conditions over tropical oceans. **Version 1.0** was released in November 1993, and included modifications to the basic LKB code for wind roughness length, Monin-Obukhov profile functions for strong convection, and low-wind "gustiness". **Version 2.0** (August 1994) included code to model the cool skin physics, and also daytime near-surface warming based on a simplified version of the Price, Weller and Pinkel (PWP) ocean mixing model. These optional features enable conversion from bulk to true skin temperature for calculating the fluxes. Calculation of fluxes of momentum and sensible heat due to rainfall are incorporated in the code, as is the so-called Webb correction to latent heat flux which arises from the requirement that the net dry mass flux be zero.

*The next major modifications to the algorithm were made at the COARE Air-Sea Interaction (Flux) Group Workshop in Honolulu, 2-4 August 1995. Transfer coefficients were adjusted by six percent to give better average agreement with covariance latent heat fluxes from several COARE ships. This produced version 2.5b, which has been used successfully on various ocean-atmosphere field campaigns by members of the Flux Group, at various locations and from a variety of platforms. At the Woods Hole workshop, 9-11 October 1996 it was agreed that no further development would be attempted to the community version of the COARE Bulk Flux Algorithm, and that a **version 2.5b** bulk algorithm "package" would be made available, consisting of the fortran source code and a test data set. This was released at a meeting of the Flux Group at NCAR, 14-16 May 1997.

*In December of 1999, Bradley and Fairall made available **version 2.6**a in both fortran and matlab forms. The new version of the model has several changes to profile functions, a simple wind-speed dependent Charnock parameter, a much simpler scalar roughness specification, a reduced stability iteration loop, and elimination of the need for a Webb correction to latent heat fluxes.

*In January of 2000, Bradley and Fairall made available **version 2.6bw** which incorporates surface gravity wave information. The data inputs have been expanded to allow three additional parameters: a switch coded 0,1, or 2 to designate the wave model used, wave period and

significant wave height. *Fig 1* illustrates the way momentum transfer is different for the different schemes in the case of fully developed waves.

wave=0: No wave model, just use the specified Charnock parameter in the version 2.6a code.
wave=1: Use the Oost et al. (2001) wave age parameterization. In this case you must specify wave period
wave=2: Use the Taylor and Yelland (2000) wave slope/height model. In this case you must specify wave period and significant wave height.

*In 2003 **version 3.0** was published (Fairall et al., 2003) and incorporates all of the modifications discussed above. The only change is another small adjustment in the warm layer and warm skin calculations. The present version of the algorithm is available in matlab and fortran at

ftp://ftp.etl.noaa.gov/et7/users/cfairall/bulkalg/cor3_0/

1.1.2 Results and Examples

Papers describing in detail Version 2.5b (Fairall et al., 1996a,b) and Version 3.0 (Fairall et al., 2003) are available as pdf. Here we will briefly show a few examples. The essence of the bulk flux scheme is the roughness length specifications or, equivalently, the 10-m neutral transfer coefficients. In *Fig. 2* we show these transfer coefficients for momentum and moisture/sensible heat; the original version 2.5 and latest version 3.0 are shown for comparison. The main difference is slightly increased momentum transfer at high winds and scalar transfer increases slightly wind speed in the newest version. The latest version is based on averaging thousands of data points; in *Fig. 3* the actual data are shown with the model. An example of the model's ability to yield the correct values, on average, for fluxes is shown in *Fig. 4* where both model-derived and measured latent heat fluxes have been composited wind speed bins (the lines denote means and the symbols denote medians). The agreement is excellent from 0 to 20 m/s. Another way to view the state of the transfer coefficients is to ratio with the Version 3.0 specifications *Fig. 5*. Here the ETL data are show as points with statistical uncertainties in the mean quantity. The dashed lines are the transfer coefficients used by the two major operational weather forecast centers (NCEP and ECMWF). NCEP recently replaced their model (labeled 'old' in the figure) with a derivative of the COARE 2.5 model. The operational parameterizations are now within 10% of the ETL data and the COARE algorithm for wind speeds from 0 to 20 m/s.

References

Fairall, C.W., E.F. Bradley, J.S. Godfrey, G.A. Wick, J.B. Edson, and G.S. Young, 1996a: The cool skin and the warm layer in bulk flux calculations. J. Geophys. Res. 101, 1295-1308.

Fairall, C.W., E.F. Bradley, D.P. Rogers, J.B. Edson, G.S. Young, 1996b: Bulk parameterization of air-sea fluxes for TOGA COARE. J. Geophys. Res. 101, 3747-3764.

Fairall, C. W., E. F. Bradley, J. E. Hare, A. A. Grachev, and J. B. Edson, 2003: Bulk parameterization of air-sea fluxes: Updates and verification for the COARE Algorithm. *J. Clim.*, **16**, 571-591.

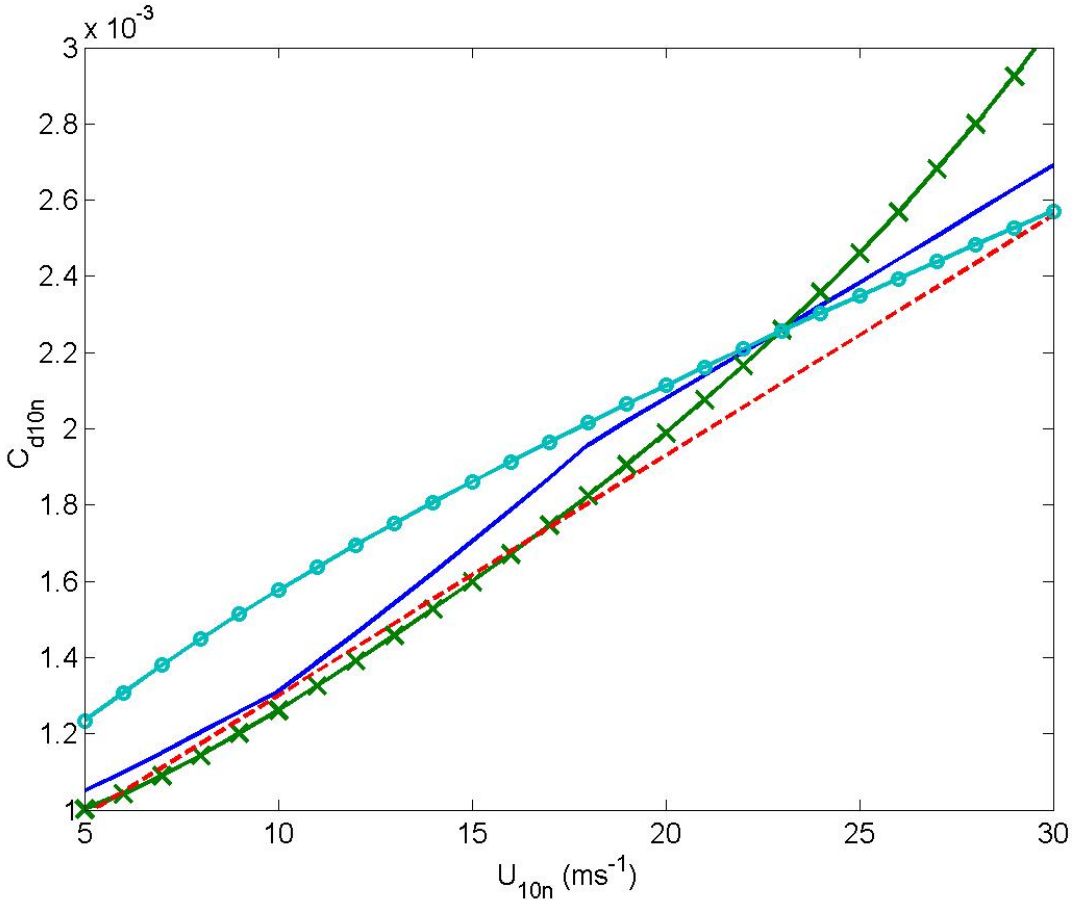

Fig. 1. Wind speed dependence of the 10-m neutral momentum transfer coefficient from several sources: solid line, COARE 3.0; dashed line, Smith (1980); line with x's, Oost et al. (2002) parameterization for fully developed seas; line with o's, Taylor and Yelland (2001) parameterization for fully developed seas.

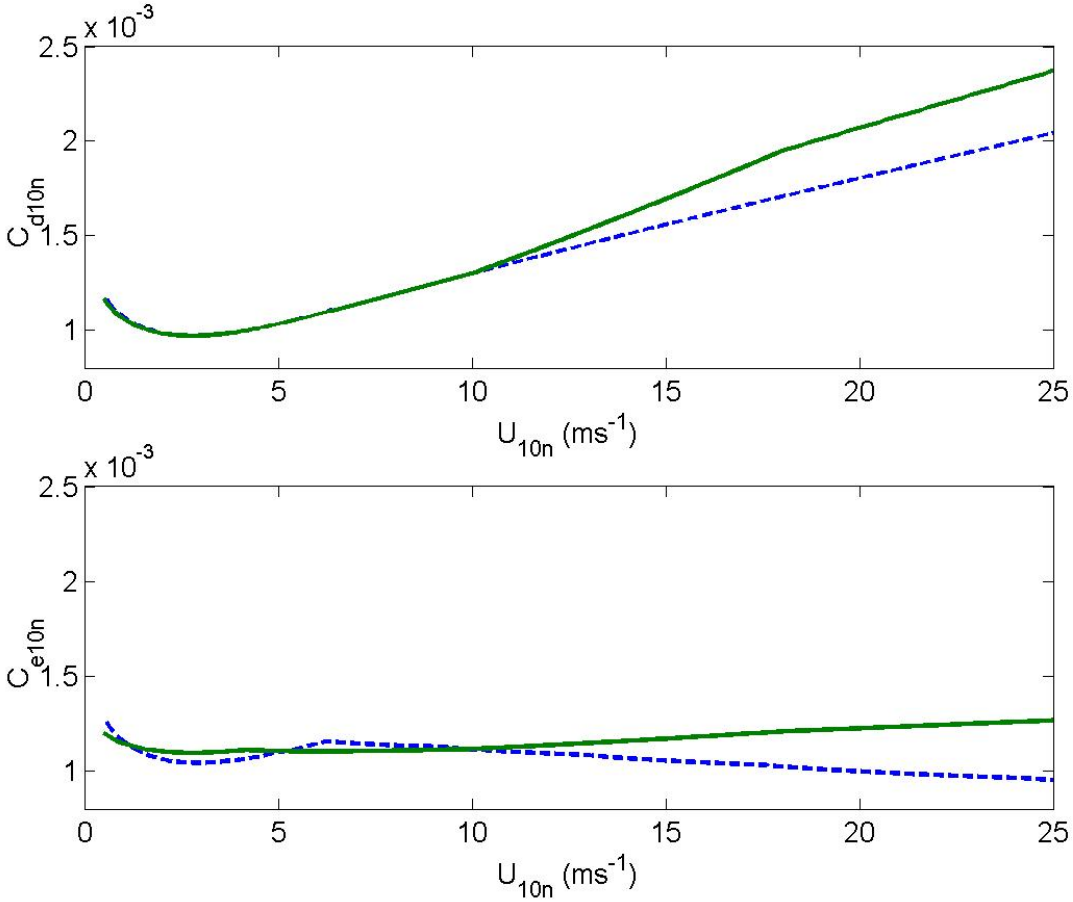

Fig. 2. Wind speed dependence of the momentum and scalar transfer coefficients for COARE versions 2.5 (broken line) and 3.0 (solid line): Upper panel, C_{d10n}; lower panel C_{e10n}.

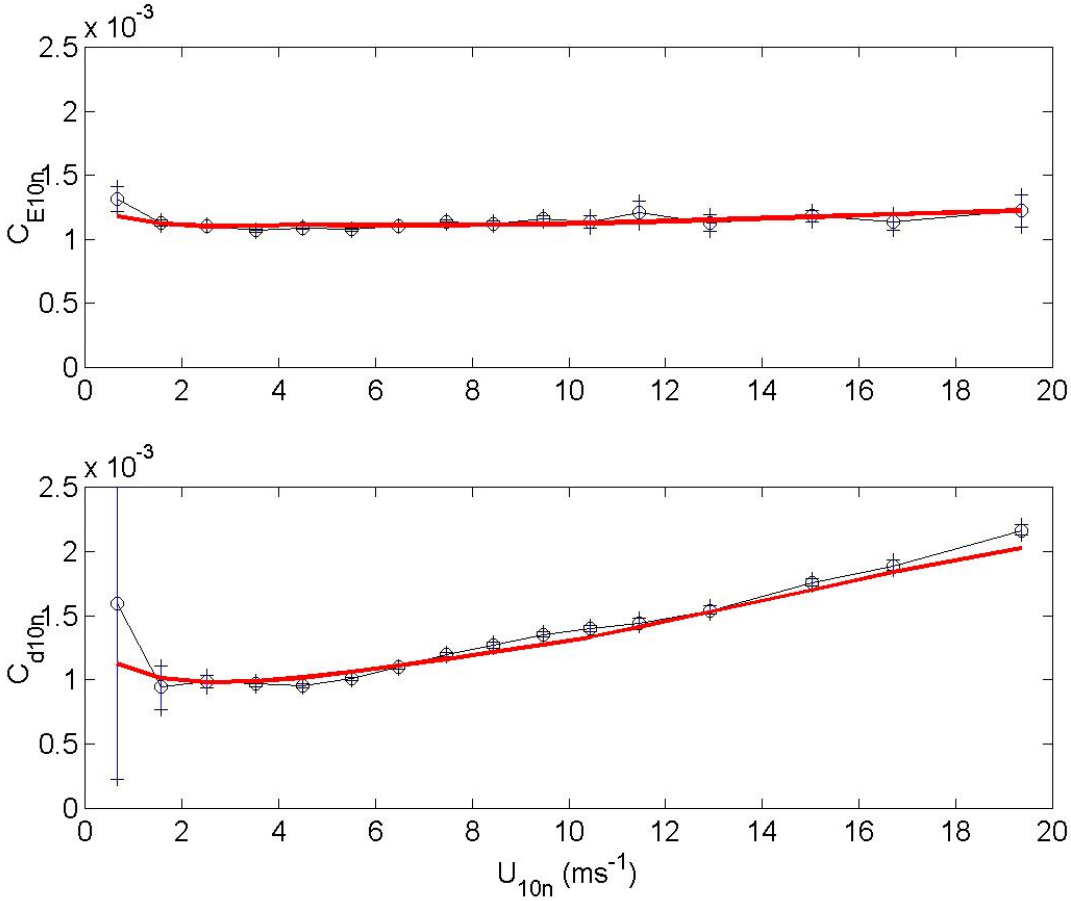

Fig. 3. Wind speed dependence of the momentum (upper panel) and scalar transfer (upper panel) coefficients for COARE versions 3.0 (solid line) and measurements (thin line with circles)

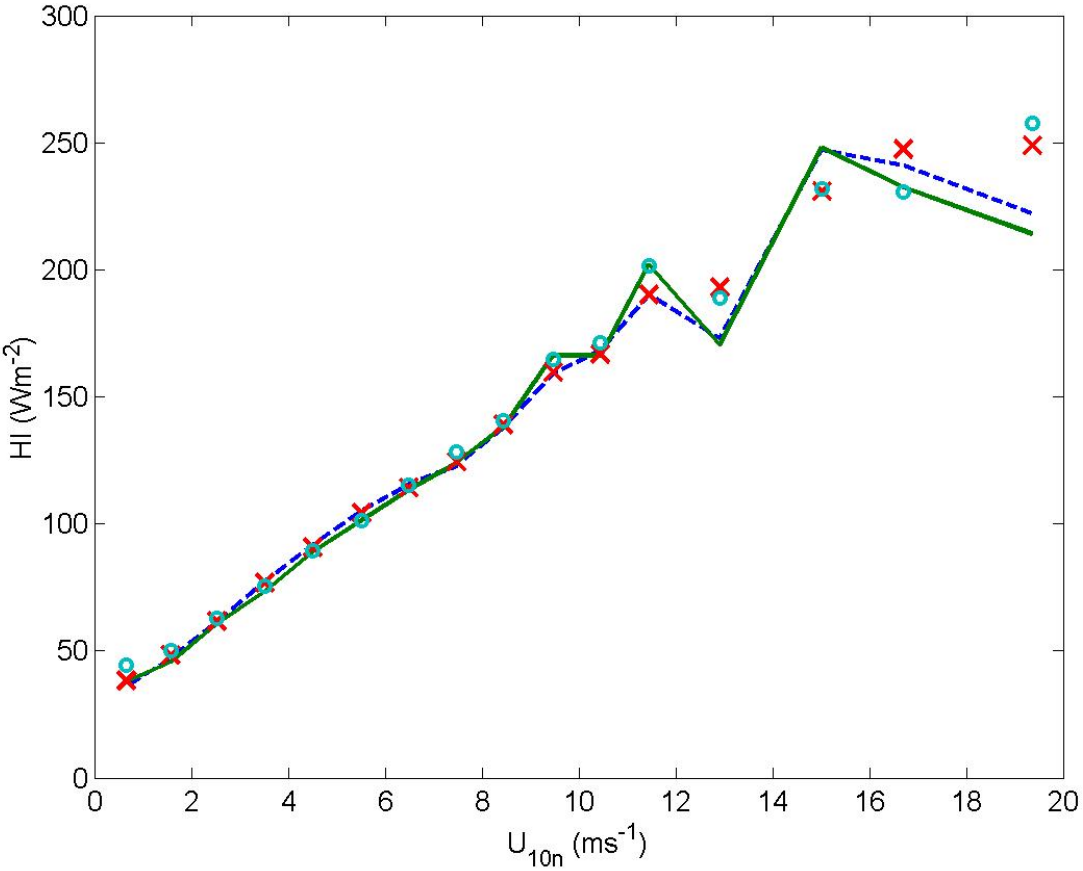

Fig. 4. The average of covariance and ID latent heat fluxes computed in 10-m neutral wind speed bins. Mean values are shown by lines and medians by symbols: the solid line and circles are measured fluxes, and the broken line and crosses are calculated with COARE 3.0.

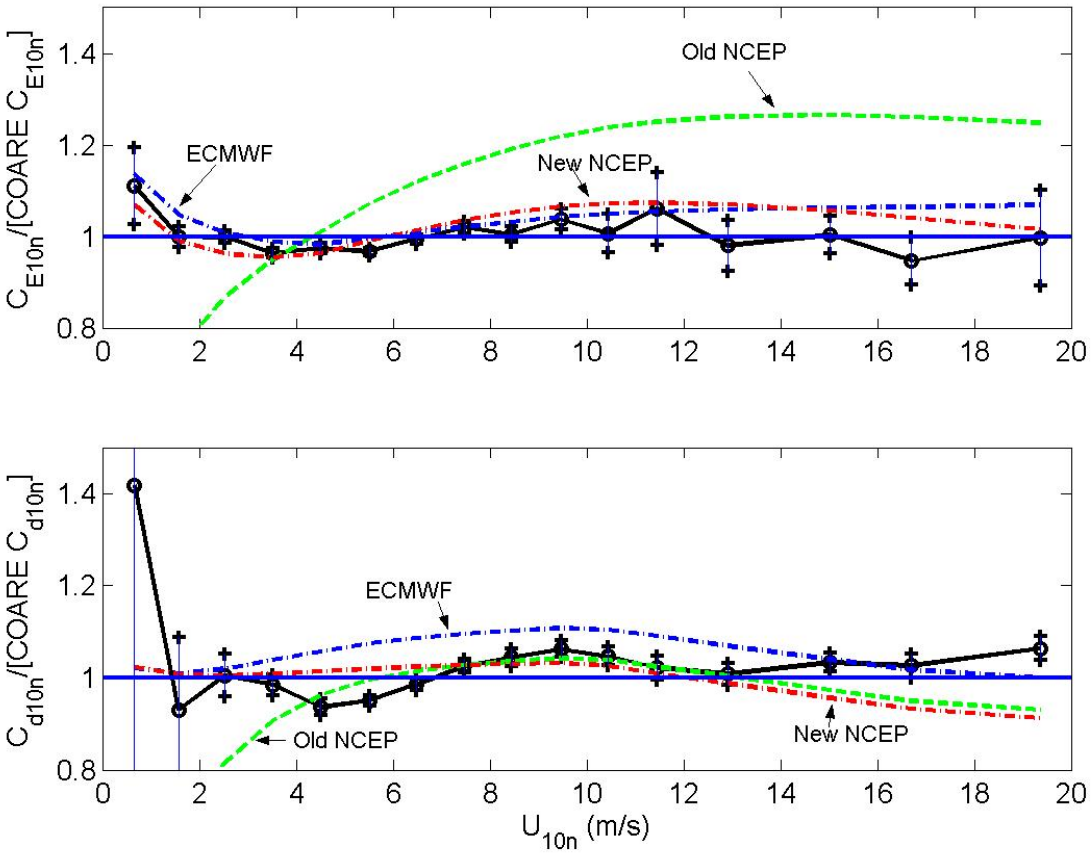

Fig. 5. The average wind speed dependence of 10-m neutral transfer coefficients divided by the COARE 3.0 values [Upper panel, C_{e10n}; lower panel C_{d10n}]. The dashed lines are NCEP and ECMWF formulae (as labeled); the solid line with symbols is the average ETL data.

1.2 Gas Fluxes

Because of the combination of small concentrations and/or small fluxes, the determination of air-sea gas fluxes present unusual measurement difficulties. Direct measurements (i.e., eddy correlation) of the fluxes are rarely attempted. In the last decade, there has been an intense scientific effort to improve measurement techniques and to place bulk parameterizations of gas transfer on firmer theoretical grounds. Oceanic tracer experiments, near-surface mean concentration profiles, eddy accumulation, and direct eddy covariance methods have all been used. Theoretical efforts have focused primarily in the realm of characterizing the transfer properties of the oceanic molecular sublayer. Recent major field efforts organized by the US (GASEX-98 and GASEX-01) and the EU (ASGAMAGE) have yielded atmospheric-derived results much closer to those from oceanographic methods. In a recent paper (Fairall et al., 2000) we reviewed the physical basis of a bulk-to-bulk gas transfer parameterization that is generalized for solubility and Schmidt number. We also discussed various aspects of recent sensor and technique developments used for direct measurements and demonstrate experimental progress with results from ASGAMAGE and GASEX-98. It is clear that sensor noise, sensitivity, and cross talk with other species and even ship motion still need improvement for accurate measurements of trace gas exchange over the ocean. Significant work remains to resolve issues associated with the effects of waves, bubbles, and surface films.

Gas transfer parameterizations are bulk flux parameterizations similar to those described above with one major difference - transfer in the ocean is more important that in the atmosphere. In the COARE algorithm, the difference in the bulk water and the interface is accounted for with the cool skin routine, which deals with molecular heat transfer across the skin layer. For transfer of most gases, this ocean skin layer resistance dominates the total bulk ocean to bulk atmospheric transfer process. A typical gas flux is represented as

$$F_c = \alpha_c k_c (f_{cw} - f_{ca}) = V_c \Delta P_c$$

Here α is the dimensionless solubility for the gas, c, k is the transfer coefficient (units of velocity), and f_w and f_a the fugacity (partial pressure) of the gas in water (subscript w) and air (subscript a). The trick, of course, is to come up with k or V_t.. Example parameterizations are shown in *Fig.6* along with data from GASEX-98. These parameterizations tend to be simple mathematical fits to data rather than representations of physical processes.

ETL has developed a physically-based parameterization of gas flux that is derived from the COARE cool-skin algorithm. It considers balance of turbulent and molecular diffusive processes in the water and air. Turbulence is generated by both surface shear (wind) and surface buoyancy (cooling) at the interface. This gas flux algorithm is described in Fairall et al. (2000) and Hare et al. (2003), but to briefly summarize the flux is expressed as

$$F_c = \frac{A_c u_{*a} \Delta P_x}{\sqrt{\rho_w / \rho_a}\,[h_w S_{cw}^{1/2} + \ln(z_w / \delta_w)/\kappa] + \alpha_c [h_a S_{ca}^{1/2} + C_d^{-1/2} - 5 + \ln(S_{ca})/(2\kappa)]}$$

where S_c is the Schmidt number (kinematic viscosity divided by the molecular diffusivity of C), z_w the reference depth (say 1 meter) in the ocean, δ_w the molecular diffusion layer thickness in the ocean, and h is a factor that expresses the balance of shear and buoyant production of turbulence. The factor $A=10^5\alpha/(RT)$ is used to express the flux in mole/m^2/s. The atmospheric terms look slightly different from the water terms because a simple parameterization of δ_a has already been inserted.

This expression can be used to examine the balance of water versus air exchange processes. Note that the water term is multiplied by the square root of the ratio of water to air density ≈ 30. In the case of carbon dioxide, the S_{cw}=650 while S_{ca}=0.9 and $\alpha \approx 1$. Thus the water side term is about 350 times larger than the air side term. Also note that the equation above only accounts for transport via turbulent-molecular processes involving the atmospheric and oceanic diffusional sublayers. Bubbles associated with whitecaps caused by breaking waves offer a parallel transport avenue. The NOAA/COARE gas flux model also incorporates a parameterization of the bubble transport component, which is added to the turbulent-molecular component. The bubble component becomes significant at wind speeds of about 7 m/s (typical whitecap threshold); at 15 m/s it is about 4 times the turbulent-molecular component.

Experimental verification and improvement in this parameterization continues through our cooperation with research groups at Woods Hole Oceanographic Institution and NOAA PMEL and AOML (McGillis et al., 2001, 2001b; Hare et al., 2003). Examples of fits of the model to field data are given in Figs 7a (GASEX98) and 7b (GASEX01). Note that the model was tuned to fit GASEX98 and does not fit GASEX01 nearly as well, especially at low wind speeds. In *Fig. 8* we use the compare the NOAA/COARE parameterization with three models

References

Fairall, C. W., J. E. Hare, J. B. Edson, and W. McGillis, 2000: Parameterization and measurement of air-sea gas transfer. *Bound.-Layer Meteorol.*, **96**, 63-105.

Hare, J. E., C. W. Fairall, W. R. McGillis, B. Ward, and R. Wanninkhof, 2003: Evaluation of the NOAA/COARE air-sea gas transfer parameterization using GasEx data. J. Geophys. Res., to appear.

McGillis, W.R., J.B. Edson, J. D. Ware, J.E. Hare, C. W. Fairall, J. H. Dacey, and R. Wanninkhof, 2001a: Carbon dioxide flux techniques performed during GasEx98. *J. Marine Chem.*, **75**, 267-280.

McGillis, W. R., J. B. Edson, J. D. Ware, J. E. Hare, and C. W. Fairall, 2001b: Direct covariance CO_2 fluxes across the air-sea interface. *J. Geophy. Res.*, **106**, 16,729- 16,746.

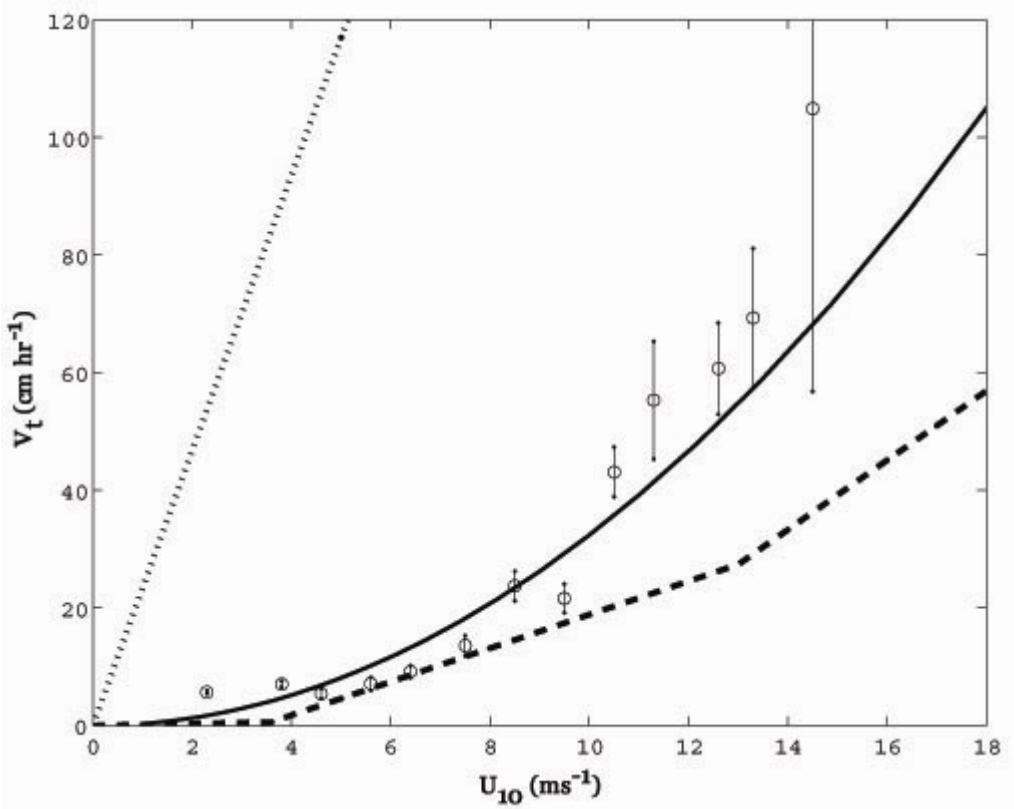

Fig. 6. CO2 transfer velocity at Sc=600 versus 10-m wind speed. The dashed line is from laboratory studies; the solid line is from Wanninkhof (1992); the circles are from GASEX-98 covariance measurements; the dotted line is an early micrometeorological result.

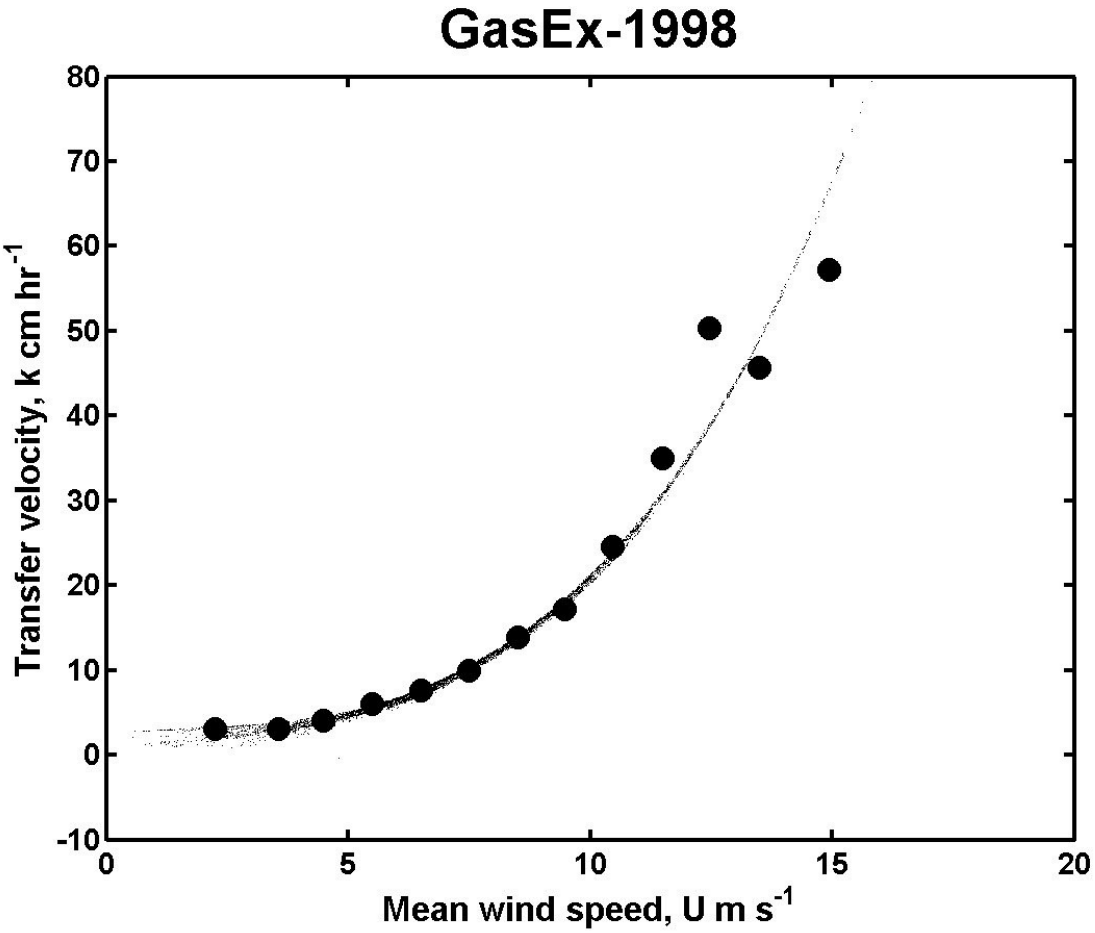

Fig. 7a. Modeled (small points) and measured (solid circles, from [12]) CO_2 transfer velocity versus mean wind speed for GasEx-1998. The NOAA/COARE gas transfer parameterization has been tuned for best fit to this data set.

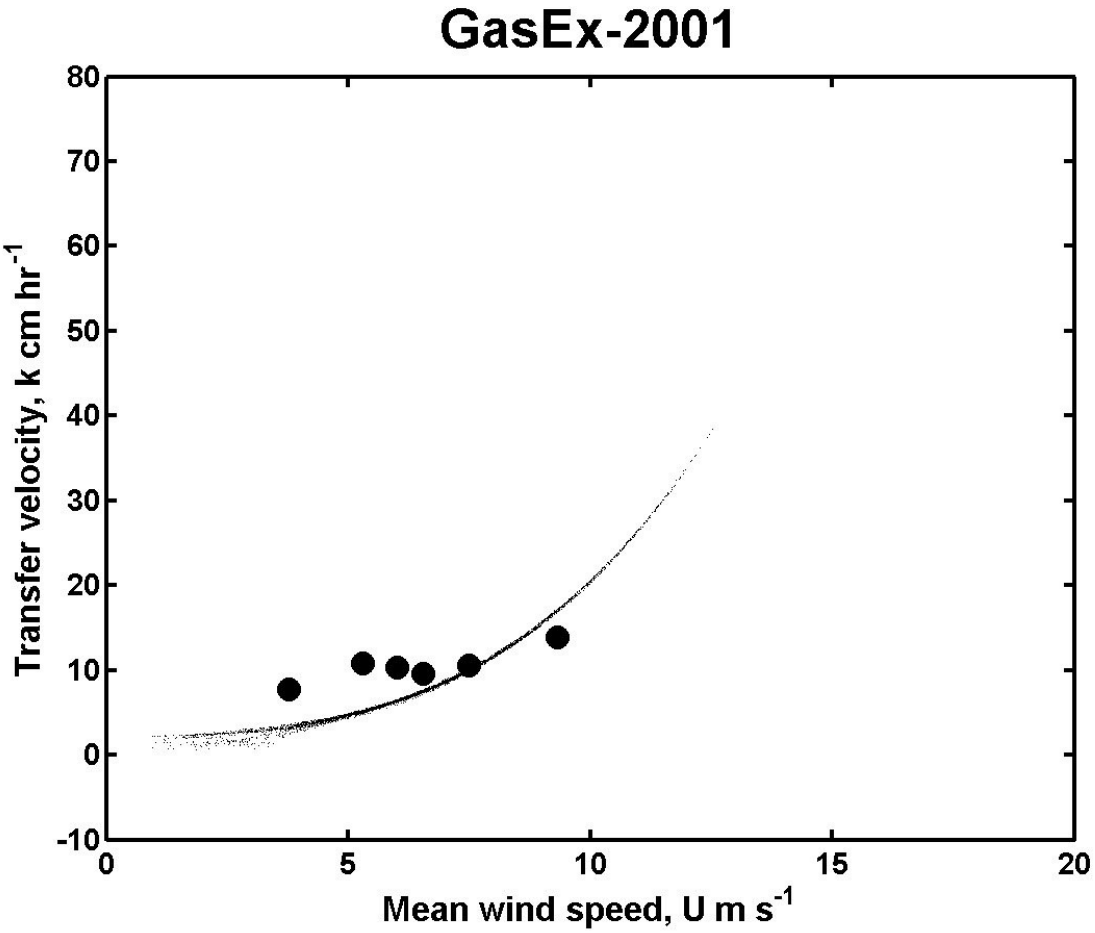

Fig. 7b. Modeled (small points) and measured (solid circles, from [12]) CO_2 transfer velocity versus mean wind speed for GasEx-2001.

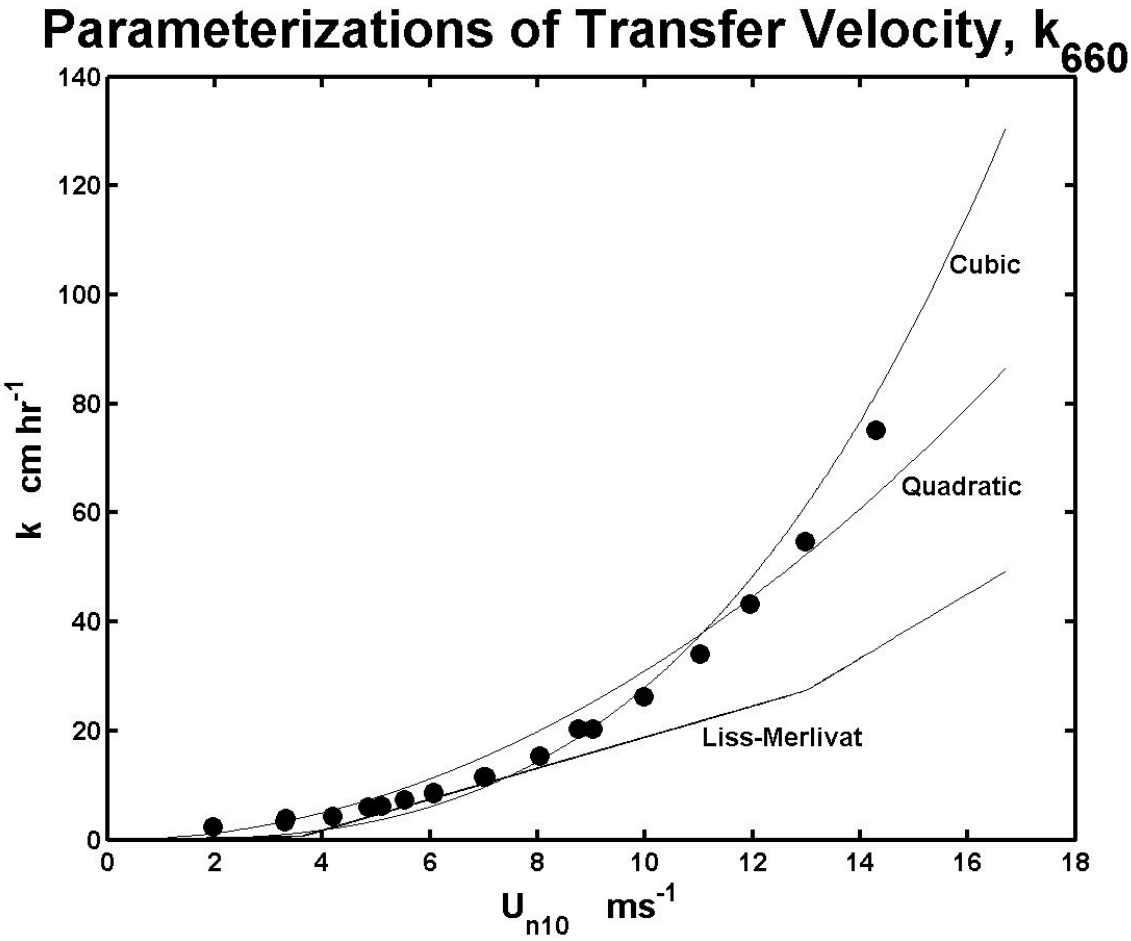

Fig. 8. Plot of the wind speed bin averaged GasEx parameterized transfer velocities, normalized to a Schmidt number of 660, versus the ten meter neutral wind speed. Also plotted are three representative wind speed only parameterizations of transfer velocity from *Wanninkhof* (1992), *Wanninkhof and McGillis* (1999), and *Liss and Merlivat* (1986).

2 *Air-Ice/Snow Fluxes*

The COARE algorithm can be applied to ice/snow covered surfaces with a few modifications: the parameterizations of the roughness lengths must be changed and the surface vapor pressure must be adjusted (for snow cover there is no suppression of vapor pressure by salinity). In computing the latent heat flux, we must account for the heat fusion (melting of ice). We have used a representation of the scalar roughness lengths from Andreas. For the SHEBA program, we used monthly varying values for z_o based on measurements. The variations were actually fairly small over the annual cycle. At present the algorithm just accounts for the fluxes realized over the ice, it does not include contributions from surrounding leads and does not handle meltponds. Based on the SHEBA results, the COARE approach works fairly well for nice flat snow covered sea ice or sea ice after the snow has melted.

3 *Air-Land Fluxes*

We have used the COARE algorithm structure on a few land-based field programs where we have direct flux measurements to determine the necessary variables to characterize the surface exchange. The preferred list of fluxes includes stress, sensible heat, latent heat, and net IR and solar radiation. The standard bulk variables are also required; we prefer upward and downward IR fluxes as a method to determine the surface temperature. Because the direct fluxes are available, the primary purpose of the bulk fluxes is to fill in gaps in the flux time series or to offer insights into comparisons with evaluation of fluxes from models (NCEP, MM5, etc).

As in the case of the ice surface, we use the COARE structure but replace the roughness parameterizations. Here we use the resistance model approach commonly used over land. The wind speed-stress relationship defines and atmospheric resistance (i.e., the inverse of conductance) to transfer, R_a

$$-\overline{w'u'} = \frac{U\kappa u_*}{\log(z/z_o) - \psi_u(\zeta)} = \frac{U}{R_a}$$

where

$$\kappa u_* R_a = \log(z/z_o) - \psi_u(\zeta)$$

The relationship between roughness length and surface type or vegetation cover os well-documented (see Fig. XX in Panofsky and Dutton, 1984). For our purposes, we normally take measurements of wind speed and stress and deduce values for zo. In some cases, this may depended on wind direction.

In the case of sensible heat transfer, we get

$$\overline{w'T'} = \frac{[T_s - \theta_a]}{R_a + R_b}$$

where

$$\kappa u_* R_b \approx \log(z_o / z_{oT}) = \log(r_r / r_T)$$

The dependence of R_b on roughness Reynolds number has been investigated in some detail and found to depend critically on the nature of the surface. For reasonably smooth surfaces, $\kappa u_* R_b$ tends to increase with r_r; for vegetation and fields of bluff roughness elements it tends to be constant with a value around 2. See the text book by Garratt (1992) for examples. Note that in light winds (smooth flow) R_b may be negative.

Finally, for evaporation we continue the analogy and write

$$\overline{w'q'} = \frac{[q_{sat}(T_s) - q_a]}{R_a + R_b + R_c}; \kappa u_* R_c = \log(z_{oT} / z_{oq})$$

Here the physical interpretation is that R_c represents the additional resistance to evaporation exerted by the plant stomates (i.e., the water vapor pressure is inside the plant and the moisture must transit the leaf stomates to reach the atmosphere). Over the ocean, swamp, or saturated ground we expect R_c to be 0; over a desert it could be very large. Whereas R_a can be straightforwardly determined experimentally, R_b is a found as a residual, and R_c as a double residual. R_c depends on the soil moisture, the type of vegetation, and is strongly influenced by radiative balances. It is essentially impossible to determine from first principles and parameterizations tend to be highly complex and not very accurate. We are not attempting to parameterize R_c at the moment, but usually determine a daily value from the direct data.

We have chosen measurements from a short field program to illustrate the implementation of the land flux model. In this example, we have a time series of measured bulk variables plus turbulent and radiative fluxes. However, the direct turbulent measurements were not available for almost half of the experiment because of problems with sensors. Thus, bulk flux calculations were used to fill in where direct data were missing.

We used the time series of stress (when available) and wind speed to estimate the surface roughness and found a value of 0.2 m. The thermal resistance was parameterized as per Garratt

$$\kappa u_* R_b = \min(2.5 R_r^{1/4} - 2, 2.0)$$

These values were then used with the time series of latent heat flux to estimate a time series of R_c. Daily mean values for R_c were saved in a lookup table and used for the entire experiment

(see *Fig. 9*). The decline of resistance to moisture transfer at the beginning of the period was caused by a rain event that greatly increased soil moisture. Another small rain event later in the period kept the values relatively low.

One way to check how well the model is doing is to use the surface energy balance

$$R_{ns} = -R_{nl} + H_s + H_l + H_g$$

where R_n are the solar (s) and IR (l) net radiative fluxes, $H_s = \rho C_p \langle w'T' \rangle$ is the sensible heat flux, $H_s = \rho L_e \langle wq' \rangle$ is the latent heat flux, and H_g is the heat flux into the ground. *Fig.10* shows the time series of R_{ns} both measured directly (line) and computed from the right hand side of the equation above (circles). *Fig. 11* shows part of the time series for the actual resistance terms. High resistance periods occur every night when the winds are lighter and the surface layer is stable. Note the resistance to moisture transfer is about 10 times that of sensible heat transfer, implying the moisture availability in the ground is significantly affecting the balance of latent and sensible heat. The actual heat balance is shown in *Fig. 12.*

References

Panofsky, H. A., and J. A. Dutton, 1984: **Atmospheric Turbulence**, Wiley-Interscience, New York, 397 pp.

Garratt, J. R., 1992: **The Atmospheric Boundary Layer**. Cambridge University Press, Cambridge, UK, 316 pp.

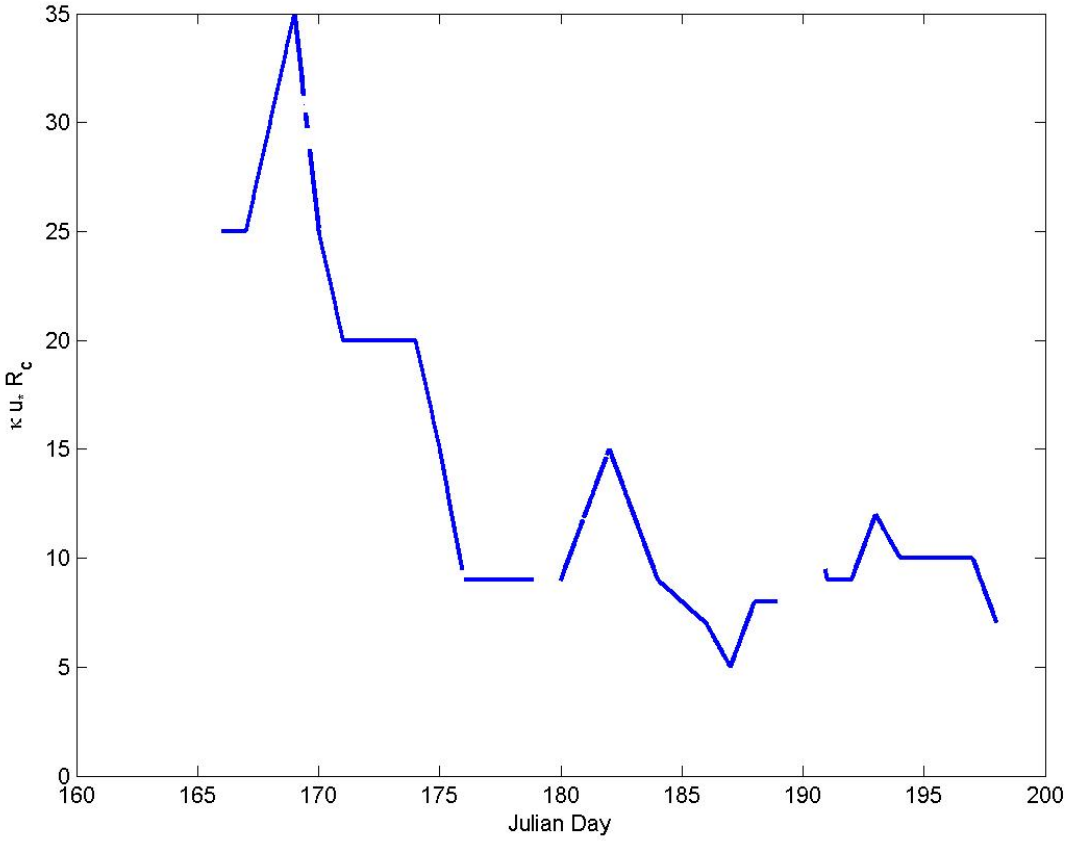

Fig. 9. Time series of moisture resistance coefficient fit to the observations of fluxes. The decreasing resistance is caused by increase in soil moisture associated with rain.

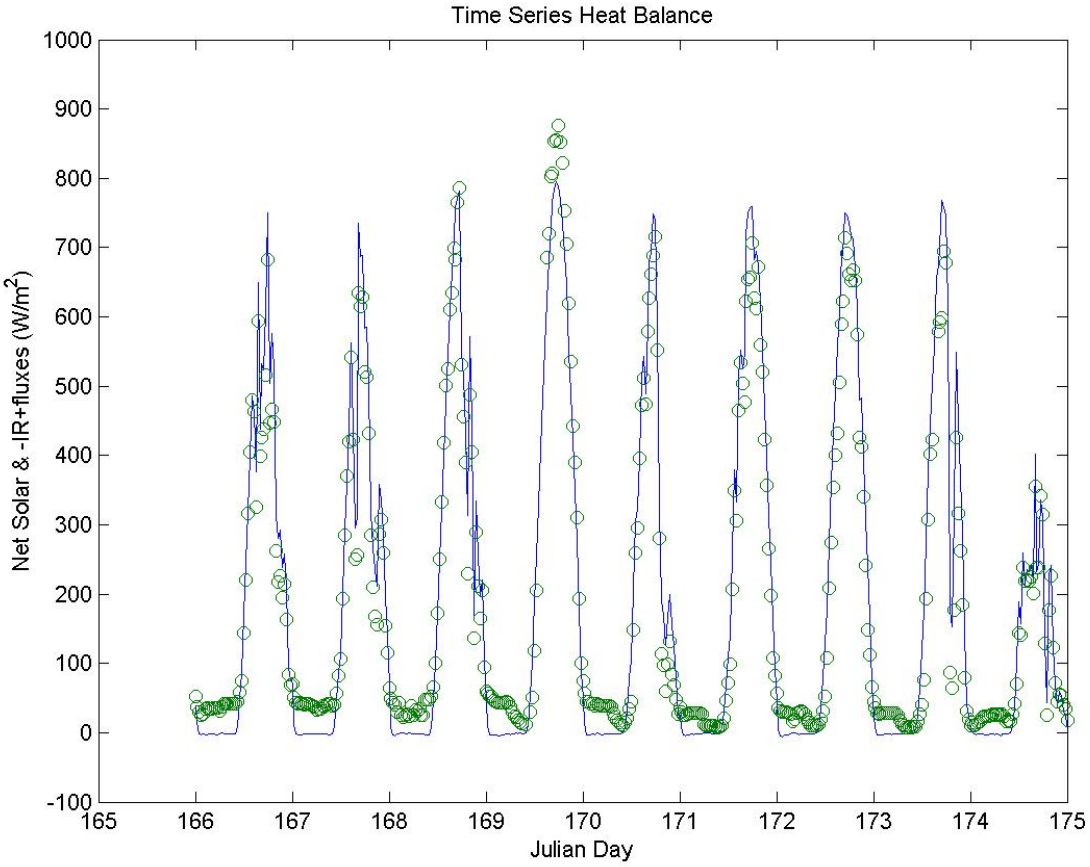

Fig. 10. Time series of the basic heat balance obtained from the bulk flux calculations. The measured net solar flux is the blue line; the sum of the various balancing components is given by the circles.

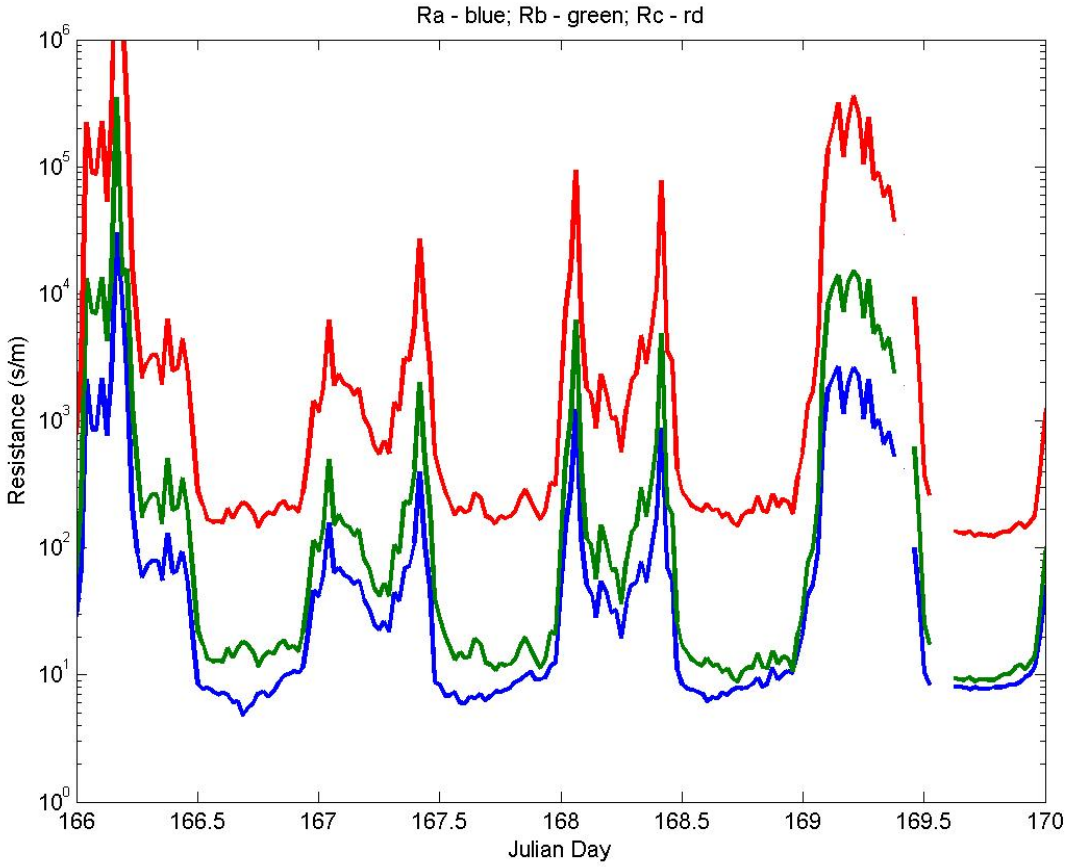

Fig. 11. Time series of the resistance terms: Ra – blue, Rb – green, and Rc – red.

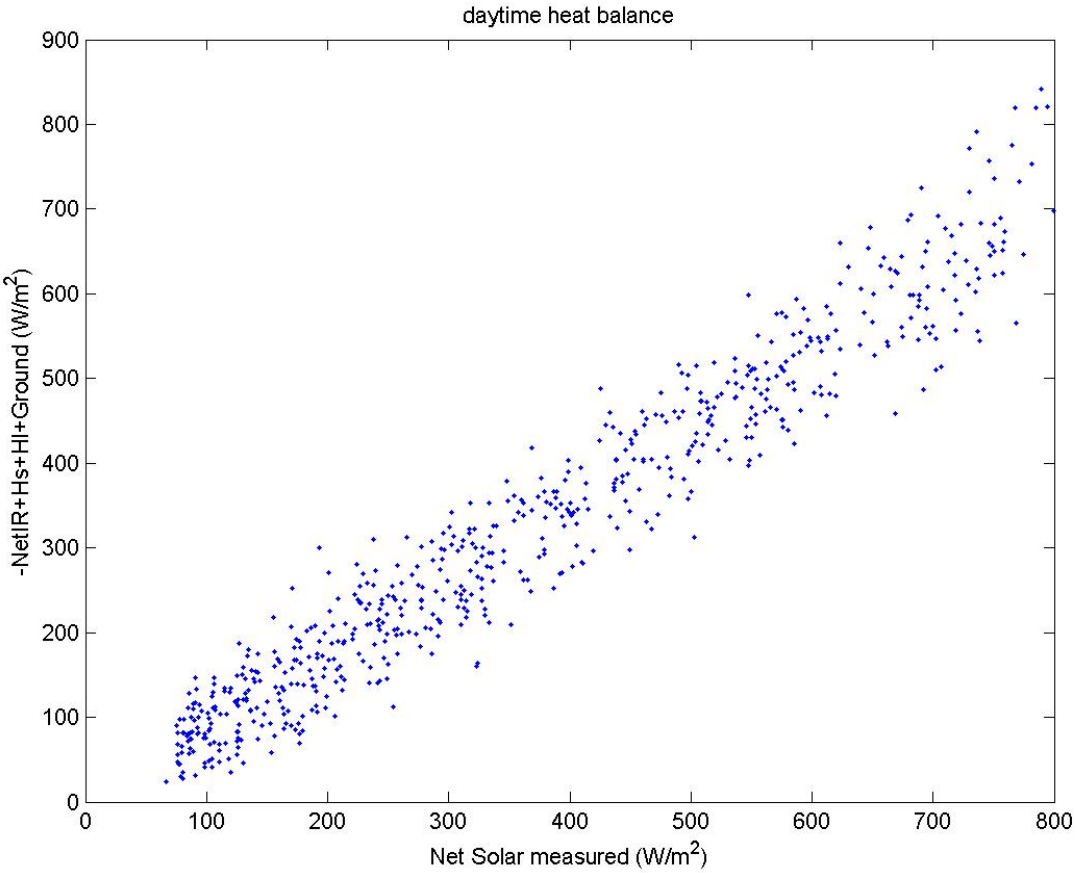

Fig. 12. The heat balance (as in Fig. 10) shown as a scatter plot: x-axis is the measured net solar flux; the y-axis the sum of the components.